Volume 18, Number 1, 2025. pp. 107-112

Jordan Journal of Physics

TECHNICAL NOTE

Exploring the Relationship Linking the Radius and Potential Difference in Hemispherical Analyzer Energy

Ataullah. A. Alsheikh Essa[a], **Khalid. Q. Kheder**[b] and **Abdullah I. M. Alabdullah**[a]

[a] *Department of Physics, College of Science, Mosul University, Mosul, Nineveh 00964, Iraq.*

[b] *Department of Medical Physics, College of Science, Mosul University, Mosul, Nineveh 00964, Iraq.*

Doi: **https://doi.org/10.47011/18.1.12**

Received on: 11/07/2023; *Accepted on: 10/12/2023*

Abstract: The development of a hemispherical energy analyzer was a part of this research and study. The instrument was specifically designed to measure the kinetic energy of electrons inside the analyzer at various energies, while the electrons' initial kinetic energy was set to remain constant before they entered the analyzer. Different mean radius values were selected for the energy analyzer to explore their influence on its performance. The relationship between the mean radius and the potential difference within the analyzer was examined, revealing an inverse correlation. As the mean radius increased, the potential difference decreased. The performance of the analyzer was assessed based on the energy resolution achieved for each radius of the hemispherical energy analyzer. The potential difference within the analyzer decreased as the mean radius increased. In addition, in the comparison of the axial electric field values along the x-axis for different values of the mean radius, it was observed that the design with the lowest value of the central radius had the highest value of the electric field. This suggests an inverse relationship between the central radius and the electric field strength along the x-axis. Furthermore, a comparison was conducted on the axial electric potential profile values along the x-axis for different mean radius values, revealing that the design with the smallest central radius exhibited the highest electric potential.

Keywords: Hemispherical energy analyzer, Radius, Potential difference.

1. Introduction

The study of electron behavior and energy distribution is crucial for understanding various phenomena in fields such as materials science, surface physics, and nanotechnology. To obtain comprehensive insights into the energy states and trajectories of electrons, researchers have developed numerous sophisticated instruments. Among these, the hemispherical electron energy analyzer has emerged as a powerful tool for characterizing electron energies and angular distributions with exceptional precision. The hemispherical energy analyzer (HEA) is extensively employed as an electrostatic energy selector in the realm of low-energy atomic collision physics and serves as a secondary stage following electrostatic lenses and electron gun systems [1, 2]. It pertains to an energy analyzer commonly utilized in surface science and condensed matter physics. Its primary purpose is to assess the kinetic energy and angular distribution of electrons released from a sample surface through diverse interactions like photoemission or electron scattering. The HEA disperses electrons based on their kinetic energy,

Corresponding Author: Ataullah. A. Alsheikh Essa **Email**: Attallah.21scp11@student.uomosl.edu.iq

akin to how a prism disperses light according to its wavelength [3].

In 1929, it was known that electrons enter the analyzer at small angles and in a cylindrical shape within a circle of radius that depends on the speed of the electrons [4]. In 1967, Kuyatt and Simpson developed a monochromatic design in which they carefully examined the slit width and electron energy [5]. Imhof (1976) measured the transit time of electrons inside the analyzer [6]. In 1979, Jost performed a simulated spherical electron spectrometer with spherical equipotential lines in the region of the beam trajectories [7]. Benis and Zouros (2008) studied the focusing and dispersive properties of an ideal 1/r [8]. Dogan *et. al.* (2013) established a relationship between the radius of the hemispherical electron analyzer and the entry potential [3]. The effects of fringing fields on the performance of the HEA have been studied by Sise and Zouros (2015) [10]. Tusche *et al.* (2019) published a research work concerning the imaging properties of hemispherical electrostatic energy analyzers for high-resolution momentum microscopy [1]

The hemispherical analyzer energy accelerates and concentrates electrons onto a position-sensitive detector using a combination of electrostatic or magnetic fields. The photoelectrons are concentrated in the analyzer and they are dispersed inside the analyzer depending on their kinetic energy and the electron beam that enters the analyzer with different energies. Particles with kinetic energies below the pass energy are deflected and do not reach the exit aperture. On the other hand, particles with kinetic energies equal to or greater than the pass energy overcome the electric field and continue along the hemispherical path, exiting through the exit aperture [3]. Each electron travels around a fixed-radius circle. The transit power voltage of the analyzer, which is the internal potential difference between the analyzer and the external voltage applied to it, is calculated.

Due to their high degree of spherical symmetry, hemispherical aberration analyzers are the energy filters with the most usage in the most recent electronic spectroscopic methods.

Indeed, careful consideration of the design aspects related to analyzer efficiency is crucial for the development of accurate and reliable spherical analyzers. By paying attention to factors such as energy resolution, transmission efficiency, energy range, electric field uniformity, signal-to-noise ratio, detector sensitivity, stability, and calibration, researchers and engineers can optimize the performance of the analyzer.

In this research, the SIMION 8.0 simulation program was used. SIMION 8.0 is a widely utilized software package for calculating electric fields given an applied potential and for simulating the trajectories of charged particles within these fields. This program is particularly effective for studying electrostatic systems, such as hemispherical electron analyzers and electron sources. [2, 10].

The analyzer consists of two concentric hemispheres with radii R_1 and R_2, which have potentials V_{in} and V_{out}, respectively, as shown in Fig. 1. The terms R_1 and R_2 refer to the inner and outer radii. R_o is the mean radius of the analyzer and denotes the path of the transit energy of the electron beam [3].

In this study, the performance of the electron energy analyzer was examined with different radii values which are obtained using the following relationship [3]:

$$R_o = \frac{R_1 + R_2}{2} \tag{1}$$

The operating characteristics including the electric field distribution (E) along the x-axis, as well as the electric potential, are calculated for each value.

If E_p, denoting pass energy, represents the kinetic energy of an electron moving within an orbit of radius R_o, the voltages applied to the inner and outer hemispheres, V_{in} and V_{out}, can be expressed as [11]:

$$V_{in,out} = V_o\left(\frac{2R_o}{R_{in,out}} - 1\right) \tag{2}$$

The two spherical electrodes that make up the hemispherical analyzer are concentrically connected to form a hemisphere respectively as shown in Fig. 1. This figure shows that electrons at the pass energy follow a path of constant radius through the analyzer, while those with lower energy approach the inner shell and those with higher energy approach the outer shell. In this way, different energies are converted into different real space positions on the microchannel plate (MCP) detector [12].

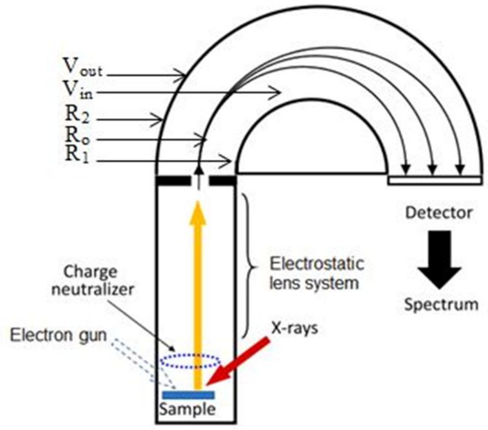

FIG. 1. Operating principle of a hemispherical electron analyzer [13].

The present research work aims to investigate the relationship between the mean radius and potential difference within the analyzer.

2. Design Considerations

When designing a hemispherical energy analyzer, numerous factors must be carefully considered to ensure optimal efficiency, accuracy, and overall performance. Among these considerations, the accuracy of energy measurement stands out as a crucial aspect. This accuracy enables the distinction between energy levels of particles, whether they are electrons or ions, within the analyzer, thereby influencing its sensitivity.

Transmission efficiency also holds significant importance in the design process. The analyzer's geometry, constituent materials, and electrical components must be meticulously selected to minimize energy loss during the transportation of particles. By addressing these factors, designers can enhance the overall performance of the analyzer.

Additionally, the energy range plays a vital role in reducing noise in the input signal. This aspect involves mitigating the effects of fringing fields, which occur when the electric field gradually diminishes away from the central region. These marginal fields can affect the behavior of particles inside the analyzer and introduce undesirable noise. By carefully managing the energy range and addressing the associated fringing fields, designers can minimize noise and optimize the performance of the hemispherical energy analyzer [14].

In this study, the design of the hemispherical energy analyzer required a careful selection of values for the inner radius (R_1) and outer radius (R_2). The mid-gap radius between these radii, denoted as R_o and illustrated in Fig. 2, was also chosen as a fixed value. This gap served as the entry point for the electron beam, which possessed a constant kinetic energy, through the analyzer's entry aperture. The electron beams then passed through the analyzer, undergoing energy analysis and exiting through the analyzer's exit aperture with modified kinetic energy.

The values of R_1 were selected as 30, 40, 50, 60, 70, 80, 90, and 100 mm. Considering that the air gap between the two hemispheres was kept constant at 18 mm, the corresponding values of R2 were 48, 58, 68, 78, 88, 98, 108, and 118 mm. Consequently, the values of Ro were 39, 49, 59, 69, 79, 89, 99, and 109 mm. These values were chosen to align with practical design constraints and to avoid fractional numbers, facilitating numerical calculations for the simulation.

The electron beam path and behavior can be controlled within the analyzer through applied voltages on the hemispherical energy analyzer electrodes. This setup allowed for precise measurements and enabled a detailed investigation of the behavior of particles with different kinetic energies.

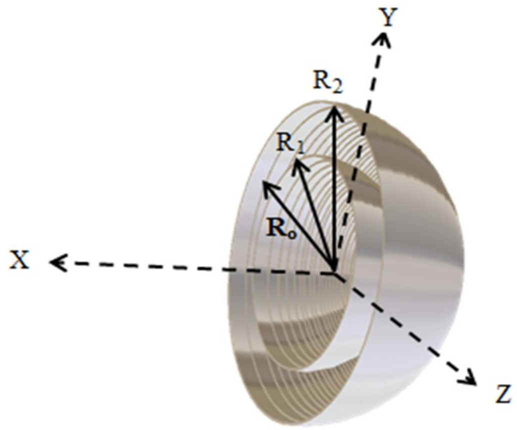

FIG. 2. Schematic representation of the HEA design showing inner, outer, and central radii (R_1, R_2, & R_o), respectively.

3. Results and Discussions

Based on electrostatic theory and the geometry of the analyzer, it is possible to define the relationship between the various radii and the potential field in a hemispherical analyzer. By applying an electric potential difference between the inner and outer surfaces of the hemisphere, the potential field inside the hemispherical analyzer is established. The electric field produced by this potential difference has an impact on the trajectory of charged particles inside the detector. The chosen values of the potential difference are based on the determination of the best value of the energy resolution that depends on the potential difference. Table 1 shows the resolution values for each potential difference.

TABLE 1. The values of the resolution values for each potential difference.

Hemispherical analyzer radius (mm)	Potential difference x 10^{-2} (Volts)	Energy resolution (mm)
39	5.25	5.91
49	4.05	7.62
59	3.35	9.05
69	2.82	10.74
79	2.45	12.29
89	2.18	13.77
99	1.97	15.34
109	1.78	17.03

It was discovered that the disparity in the net internal and external potential difference applied to the hemispherical energy analyzer exhibits an inverse relationship with the rise in the central radius of the electron path. Consequently, as the central radius of the analyzer increases, the gap between the applied potential differences decreases.

The mathematical relationship between the potential difference and the radius of the hemispherical analyzer for energy can be expressed as follows:

$\Delta V \propto 1/R_o$

where ΔV represents the difference in electric potential and R_o represents the mean radius of the hemispherical analyzer.

This relationship suggests that as the radius of the analyzer increases, the difference in potential difference decreases. Conversely, a smaller radius results in a greater potential difference. Understanding this relationship is important for analyzing and interpreting the data obtained from the hemispherical energy analyzer. It helps researchers adjust the applied potential difference to achieve precise energy measurements and optimize the analyzer's performance.

$$\Delta V = \frac{2}{R_o} \quad (3)$$

The axial potential distribution (V_x) was calculated for each mean radii (R_o =39, 49, 59, 69, 79, 89, 99, and 109 mm) while applying the corresponding potential differences to the inner and outer electrodes, as shown in Fig. 3. These calculated values are represented in Fig. 4, which demonstrates that the potential initially increases to a maximum before rapidly decreasing. Additionally, the peak potential values decrease as R_o increases.

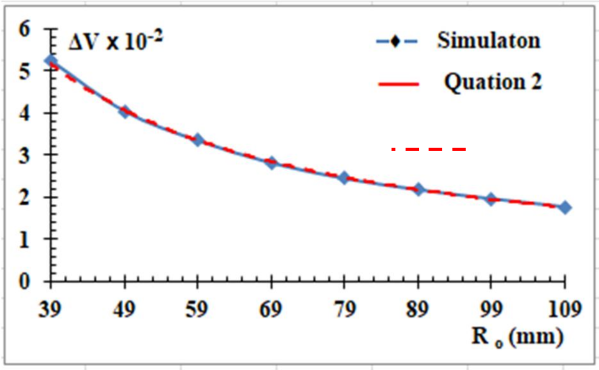

FIG. 3. Variation of the potential difference due to the changing of the mean radius of the hemispherical analyzer for the R_o = 39, 49, 59, 69, 79, 89, 99, and 109 mm.

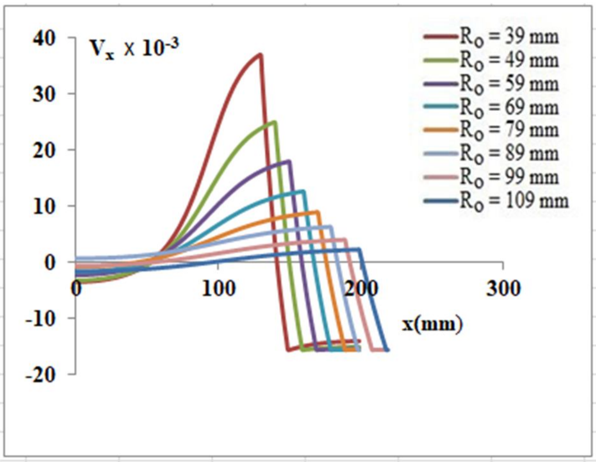

FIG. 4. Comparison of the axial electric potential (V_x) for mean radius values R_o = 39, 49, 59, 69, 79, 89, 99, and 109 mm calculated at ΔV=5.25, 4.05, 3.35, 2.28, 2.45, 2.18, 1.97, and 1.78 V, respectively.

The distribution of the axial field (E_x) was computed for various mean radii (R_o =39, 49, 59, 69, 79, 89, 99, and 109 mm) of the HEA. During these calculations, the field differences on the outer and inner electrodes were applied based on the corresponding values shown in Fig. 3.

The results of these calculations are presented in Fig. 5. The figure illustrates that the axial field values initially increase to a maximum before rapidly declining. Furthermore, it is observed that the maximum axial field values decrease as the mean radius (R_o) increases.

.

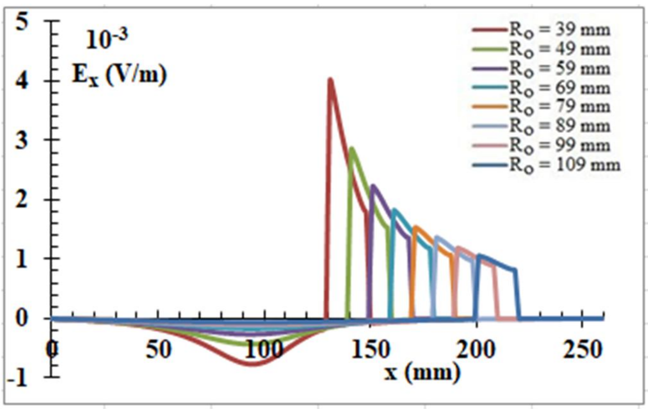

FIG. 5. Comparison of the axial field distribution (E_x) for R_o =39, 49, 59, 69, 79, 89, 99, and 109 mm) calculated at ΔV=5.25, 4.05, 3.35, 2.28, 2.45, 2.18, 1.97, and 1.78 V, respectively.

4. Conclusion

This research focused on developing a hemispherical energy analyzer device and investigating the relationship between the mean radius and voltage difference. The study revealed an inverse correlation between the voltage difference and the mean radius. The design with the smallest central radius exhibited the highest electric field strength, indicating an inverse relationship between the central radius and the electric field along the x-axis. A mathematical relationship ($\Delta V = 2/R_0$) was established to quantify the relationship between the mean radius and the applied voltage difference. These findings contribute to the optimization of hemispherical energy analyzers in scientific applications.

References

[1] Tusche, C., Chen, Y.J., Schneider, C.M., and Kirschner, J., Ultramicroscopy, 206 (2019) 112815.

[2] Alabdullah, A.I., Optik, 268 (2022) 16976.

[3] Dogan, M., Ulu, M., Gennarakis, G.G., and Zouros, T.J.M., Rev. Sci. Instrum., 84(4) (2013) 043105.

[4] Hughes, A.L. and Rojansky, V., Phys. Rev., 34(2) (1929) 284.

[5] Kuyatt, C.E. and Simpson, J.A., Rev. Sci. Instrum., 38(1) (1967) 103.

[6] Imhof, R. and King, G.C., J. Phys. E, 9(2) (1976) 138 .

[7] Jost, K., J. Phys. E, 12(10) (1979) 1001.

[8] Benis, E.P. and Zouros, T.J.M., J. Electron Spectrosc. Relat. Phenom., 163(1-3) (2008) 28.

[9] Sise, O. and Zouros, T.J., J. Spectrosc., 2015 (2015) 1.

[10] Dahl, D.A., Int. J. Mass Spectrom., 200(1-3) (2000) 3.

[11] Sise, O., Ulu, M., and Dogan, M., Nucl. Instrum. Methods Phys. Res., Sect. A, 554(1-3) (2005) 114.

[12] Dogan, M., Sise, O., and Ulu, M., Radiat. Phys. Chem., 76(3) (2007) 445.

[13] Greczynski, G. and Hultman, L., Prog. Mater. Sci., 107 (2020) 100591.

[14] Sise, O., UPB Sci. Bull., Ser. A, 77 (2015) 213.